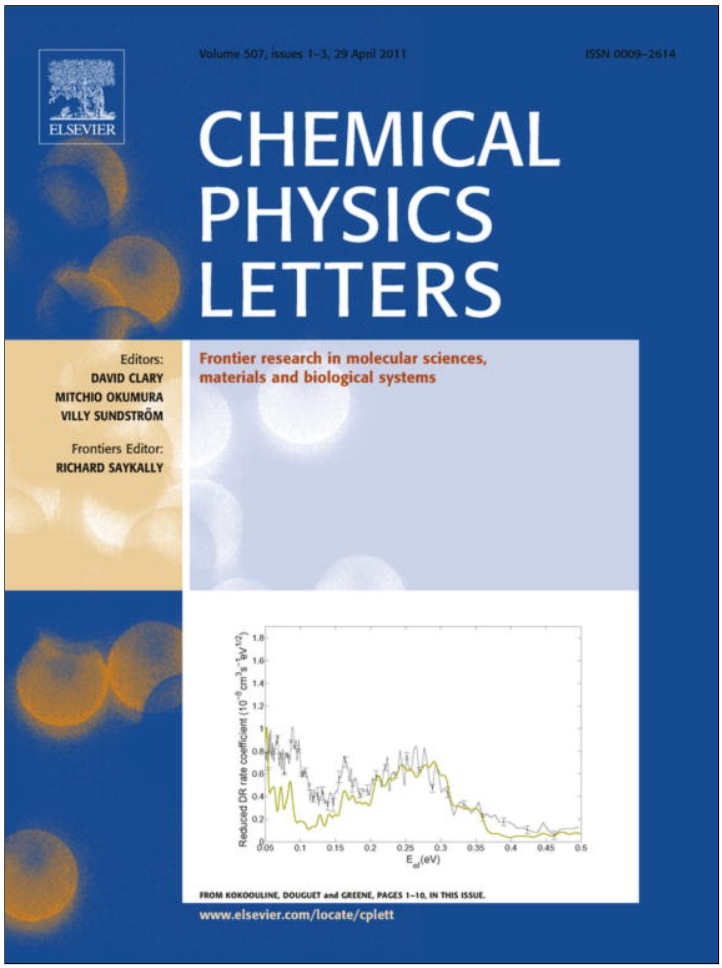

Chemical Physics Letters 507 (2011) 174–177

Contents lists available at ScienceDirect

Chemical Physics Letters

journal homepage: www.elsevier.com/locate/cplett

Modeling the diiron(II) ferroxidase complex in human H ferritin

Daniel E. Bacelo [a,b], R.C. Binning Jr. [a,*]

[a] Department of Sciences and Technology, Universidad Metropolitana, P.O. Box 21150, San Juan, PR 00928-1150, USA
[b] Dpto. de Química, FCN, Universidad Nacional de la Patagonia San Juan Bosco, Km. 4, (9000) Comodoro Rivadavia, Chubut, Argentina

ARTICLE INFO

Article history:
Received 31 January 2011
In final form 24 March 2011
Available online 11 April 2011

ABSTRACT

Density functional theory calculations, in both the high-spin and broken symmetry approximations, have been conducted on models of the diiron(II) ferroxidase complex of human H ferritin. Initial configurations were chosen from previous experimental and theoretical structures of the dizinc complex. The diiron complexes show no significant deviation in ligand or metal positions from the corresponding dizinc complexes, even maintaining similar structures through an extensive reorganization, and thus the often-made assumption of homology between Fe(II) and Zn(II) is supported. Geometry differences between diiron complexes calculated in the high-spin and broken symmetry approximations are also found to be minor.

1. Introduction

A recent computational examination of the dizinc(II) ferroxidase complex in the iron-storage protein human H ferritin (HuHF) [1] succeeded in identifying the ligands missing from the crystallographic structure [2] and completely defining the coordination environments of the metal ions. However, the function of the ferroxidase center in vivo is to bind a pair of Fe(II) ions, and the diiron complex is therefore inherently more interesting than the dizinc. The present work examines the structures of diiron complexes derived by replacing Zn with Fe in both the incomplete dizinc experimental ferroxidase structure and in the calculated best fit to the experimental structure. The latter is of interest because it directly provides a plausible model of the diiron complex, provided the dizinc and diiron structures are homologous. In the former, because three ligand positions are unoccupied, optimization of the dizinc complex resulted in reorganization [1], and substituting iron thus provides a dynamical test of the Fe–Zn homology.

Ferritins are the principal iron storage proteins in animals, plants and bacteria [3,4]. Animal ferritins consist of 24 subunits of two types, H and L, that assemble as a hollow sphere. Although subunit length and sequence vary considerably across species, three-dimensional structure is well conserved. Within each H subunit is a ferroxidase center at which two Fe(II) ions are bound, at sites conventionally labeled A and B, and oxidized by a single O_2 to an Fe(III) oxide hydrate that is subsequently transported from the center to be stored in the central cavity of the protein. The thermochemistry and kinetics of initial iron binding in HuHF have been intensely studied [5,6], and the structure of the resulting diiron(II) intermediate is thus important in interpreting the early mechanism of the ferroxidase reaction.

Crystals of ferritin with Fe(II) in the ferroxidase center have not yet been obtained, but bound metal complexes have been crystallographically imaged with substitute cations. Zn(II) is assumed to be a good substitute for Fe(II) in structure determination of complexes of the latter because it is redox stable, the ions are similar in size and both are moderately Lewis acidic [7]. Zn(II) has been employed in studies of ferroxidase complexes in HuHF [2], human mitochondrial ferritin [8] and *Escherichia coli* nonheme ferritin [9]. Other cations have also been employed with HuHF [10] and other ferritins.

The amino acids essential to ferroxidase activity have been identified by a combination of kinetics and site-directed mutagenesis [11]. These have been shown to provide the basis for an effective model of the ferroxidase center [1]. In HuHF the necessary complement of amino acids includes Glu27, Glu62 and His65 at site A and Glu107, Gln141 and Ala144 at site B. The complete atomic structures of each residue are employed and all float during optimization, except the four atoms that participate in the amide-bonded protein backbone. These are fixed in their experimental positions to maintain their spatial relationship, and dangling bonds are capped with hydrogen atoms. The model has been tested and shown to be able accurately to reproduce the structures of ferroxidase complexes. In the case of dizinc ferroxidase the model accurately matched the experimental structure, identifying the coordination orientations of the ligands, even those missing from the crystallographic structure.

In HuHF dizinc ferroxidase a water oxygen was imaged at site A in the crystal structure of the wild-type center [2], bringing the number of known ligand positions to four. Coordination of five is presumed because open positions must be available to bind O_2, and both experimental [12] and computational [13] studies

* Corresponding author. Fax: +1 787 759 7663.
E-mail addresses: binningrc@yahoo.com, um_dbacelo@suagm.edu (R.C. Binning Jr).

0009-2614/$ - see front matter © 2011 Elsevier B.V. All rights reserved.
doi:10.1016/j.cplett.2011.03.083

confirm pentacoordination. With one position at site A to be occupied, direct computational search became feasible. However, optimization of the experimental complex resulted in dissociation of the water molecule to form a hydroxide bridge and a protonated glutamate. The hydroxide bridge provided the fifth ligand at site A, once a water molecule was restored at the experimental position, and the fourth at site B. A geometry search then assigned the fifth ligand, a water molecule, at site B, and the structure of the dizinc complex was complete [1].

Several factors motivate the work discussed herein. First it is important to have a structure for the diiron(II) ferroxidase complex. The complex reacts with O_2, a crucial step in the reaction, and understanding the mechanism of the ferroxidase reaction requires knowing the reactant structure. A single structure is probably insufficient to characterize the ferroxidase complex because both experimental and theoretical studies [2,10,13] show that a number of relatively low-energy structures are accessible. Nevertheless an empirically-based structure provides a valid model upon which to found mechanistic arguments from which to begin to explore alternative structures. Further motivation for the research is grounded in the need to know whether the Zn and Fe complexes are structurally similar enough to warrant the assumption of homology between the two that is often made. It is an assumption that receives few direct tests. Finally it is important to examine the effect on calculated geometries of the two common spin state representations applied in density functional theory calculations on diiron complexes that display weak antiferromagnetic coupling, the high-spin (HS) and the broken symmetry (BS) approximations.

Zn(II) is a closed-shell singlet, whereas each iron in the diiron(II) ferroxidase complex is high-spin, its singlet electronic state formed by the spins of the two metal centers being opposed, antiferromagnetic coupling. The available spectroscopic data support this view [12]. In density functional theoretical (DFT) calculations on such states two approaches are taken. The entire system may be treated as if ferromagnetically coupled, overall high spin, thereby keeping a pure spin state that is well represented as a single electronic configuration. The error arising from the fact that the wrong electronic state is used is assumed to be small because the two high-spin centers are maintained and the coupling between them is a weak perturbation. Alternatively a calculation may be performed in which opposed spin densities are created on the individual ions, in which case the spin symmetry is sacrificed, but physically realistic spin density is retained. This is the broken symmetry approach [14]. Both approaches have been shown to be able to represent experimental geometries of diiron complexes accurately [15,16]. In the Heisenberg spin-coupling approximation the high-spin and broken symmetry energies are related by [14].

$$E_{HS} - E_{BS} = -4JS_1S_2 \quad (1)$$

where J is the coupling constant. Once J is known the ladder of spin states may be obtained, the ground state being then

$$E_0 = E_{HS} + JS_{max}(S_{max} + 1) - JS_{min}(S_{min} + 1). \quad (2)$$

2. Methods

Energies were obtained in spin-unrestricted density functional theory calculations with the BPW91 functionals. BPW91 employs Becke's 1988 exchange functional [17] and the gradient-corrected correlation functional of Perdew and Wang [18]. Numerical basis sets of double numerical plus polarization quality (DNP) were employed. This combination of functionals and basis sets has been shown effective in accurately describing the structures of diiron complexes [15,16]. Calculations were carried out with the Dmol^3 program [19,20].

3. Results and discussion

The crystallographic structure of wild-type HuHF dizinc ferroxidase complex [2] is displayed in Figure 1 with hydrogen atoms added. The Zn at site A is coordinated to one O from Glu27, one O from Glu62, one O presumed to be from a molecule of water and an N from His65. Zn at site B is coordinated to both carboxylate Os of Glu107 plus the second O of Glu62, which bridges the two sites. The formamidyl O of Gln141 is seen to be positioned pointing toward the midpoint of the two metal ions, though it is some 3.5 Å distant. As discussed above it was the identification of the site A water ligand in the crystallographic structure that made computational completion of the structure feasible. The computational study [1] identified a hydroxide bridge between sites A and B, another water molecule at site B and showed that no other ligand or peripheral molecules are present in the experimental dizinc ferroxidase center. The position of the Gln141 oxygen atom midway between the metal ions was explained with the revelation of the hydroxide bridge, which hydrogen bonds to that atom (see Figure 2).

A direct test of how closely the Fe and Zn complexes resemble each other was obtained by replacing Zn(II) with Fe(II) in the calculated dizinc ferroxidase complex that best fits the experimental atomic positions. The Fe(II) complex, Compound 1 in Table 1, was optimized in both the high-spin and the broken symmetry models, and it is displayed in Figure 2. The structure is so similar to that of the zinc complex that the assumption of homology is fully supported. The mean absolute deviation between all atoms in the diiron complex in the broken symmetry approximation and the dizinc counterpart was only 0.050 Å, with a maximum deviation of 0.22 Å; the maximum was in an oxygen atom of one of the water molecules. Deviation between the zinc and high-spin iron complexes was slightly greater, 0.087 Å, and the maximum deviation was 0.28 Å. The zinc and iron complexes are shown superimposed in Figure 3, and the near identity in structures is readily apparent. The Zn–Zn distance is 3.41 Å, the broken symmetry Fe–Fe is 3.42 Å and the high-spin Fe–Fe is 3.43 Å.

The assembly energy from amino acids, metals and water molecules of the diiron complex is found to be less than that of the dizinc complex by 12 kcal/mole (Table 1). This is consistent with observations that Zn(II) is an inhibitor of iron uptake in HuHF, although it must be noted that the major source of inhibition appears to be associated with sites in the threefold channel leading

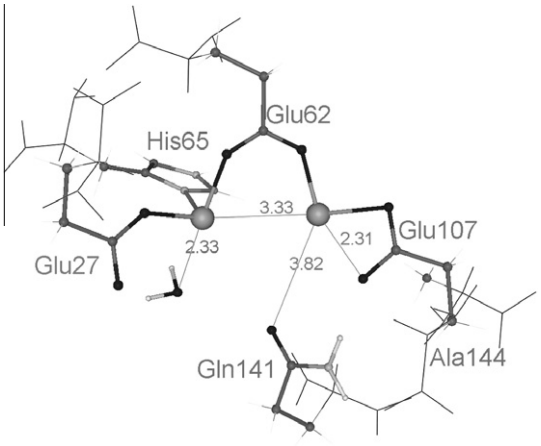

Figure 1. Experimental configuration [2] of the dizinc ferroxidase model center with component amino acids labeled. Oxygen atoms are black, carbons darker gray, nitrogens lighter gray, hydrogen atoms lighter and smaller and zinc ions medium gray and larger.

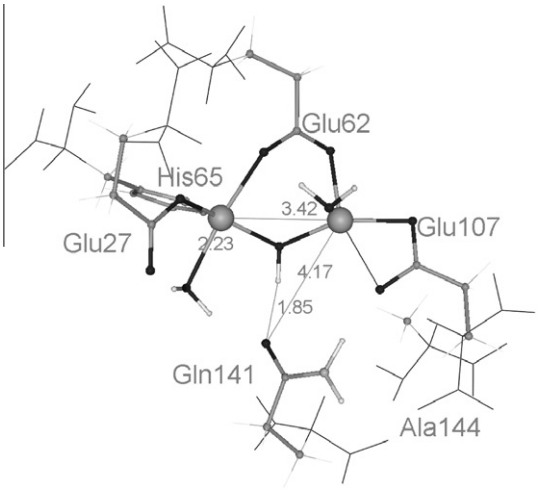

Figure 2. The diiron(II) ferroxidase complex resulting from BPW91/DNP broken symmetry optimization of the best-fit dizinc complex with Zn ions replaced by Fe. Coordination at site A is approximately trigonal bipyramidal, while at site B it is more nearly square pyramidal. The water molecule at site B sits above the plane of the zincs and the Glu62 carboxylate group.

Table 1
Total energies (in a.u.) of complexes and their components discussed in the text.

Compound	E_0	E_{HS}	E_{BS}
Fe^{2+}	−1262.91 164	−1262.91 164	
H_2O	−76.46 035		
OH^-	−75.79 970		
Glu27	−475.98 262		
Tyr34	−554.92 173		
Glu62	−475.98 232		
His65	−473.65 696		
Glu107	−475.98 264		
Gln141	−456.64 919		
Ala144	−248.56 560		
1-Opt from best fit geom	−5363.47 756	−5363.47 390	−5363.47 683
2-Opt from exptl geom	−5210.93 316	−5210.92 183	−5210.93 089
3-Tyr34 added to 2	−5918.40 307	−5918.39 922	−5918.40 230

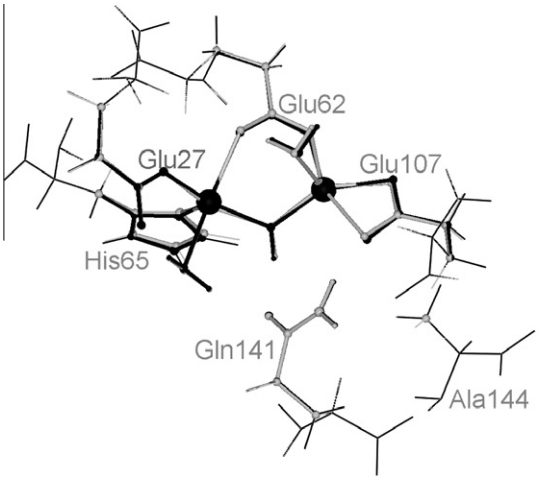

Figure 3. The diiron complex of Figure 2 (gray) superimposed on the dizinc complex from which it was derived (black), to illustrate the close agreement between the structures.

to the ferroxidase center rather than in the center itself [21]. The exchange coupling constant J, obtained from Eq. (1), was $-124\ cm^{-1}$, typical of such complexes [15,16], and confirming the assumption of weak coupling between centers.

Replacing Zn with Fe in the experimental structure shown in Figure 1 provides a different test of the functional similarity of the complexes of the two metals. Because two ligands occupying three ligand positions are actually missing from the structure, direct computational optimization of the dizinc complex resulted in considerable reorganization, including dissociation of the water molecule to form a hydroxide bridge between sites. The reaction is impelled by the exothermicity of the hydroxide bridge formation, which is greater than 44 kcal/mole. Therefore reoptimization of the Figure 1 structure with Fe in place of Zn provides not only a single structure comparison but actually a comparison of a sequence of structures along the reaction path.

The optimized high-spin and broken symmetry diiron structures, Compound 2 in Table 1, varied somewhat more from each other and from the dizinc than was the case with the previously discussed replacement calculations. Metal–metal distances ranged from 3.11to 3.24 Å, whereas they were essentially identical in the optimizations of Compound 1. However, the final structures still closely match each other, and closely similar paths to the final structures were taken in each calculation. The hydroxide bridge formed, and Glu27 was protonated. The overall mean absolute deviation of the atomic positions of the iron structures from the zinc was less than 0.2 Å in both cases.

A final structural comparison was made by adding Tyr34 to the basic model. The absence of Tyr34 has been shown to slow the ferroxidase reaction in some ferritins [22] and its addition to the basic model slightly improved the agreement between the calculated and experimental structures of the dizinc ferroxidase complex [1]. This latter effect appears to be due to the fact that a hydrogen bond from Tyr34 to one of the carboxylate Os of Glu107 inhibits rotation of the carboxylate group. Once again Fe was substituted for Zn in the best-fit structure. The optimized structure is Compound 3 in Table 1. Tyr34 did not, however, significantly improve agreement of either the high-spin or broken symmetry diiron structures with the dizinc. Although the mean absolute deviation in atomic positions between the high-spin diiron complex and the dizinc did improve from 0.087 Å without Tyr34 to 0.075 Å with, the deviations in the broken symmetry case were slightly higher, and in both cases the maximum deviation was also slightly higher.

4. Conclusions

This study affirms the assumption that Zn(II) is an appropriate substitute in structure determinations of organoiron complexes in general and ferritin ferroxidase in particular. The structures of the diiron and dizinc complexes match closely, and replacement of zinc by iron in a complex that rearranges considerably results in similar rearrangement and final structure. Thus the results of this study support the view that crystallographic imaging of the dizinc ferroxidase has yielded an accurate model of the diiron complex. In addition the high-spin and broken symmetry approximations to antiferromagnetic coupling yield essentially indistinguishable structures.

The structure of the HuHF diiron(II) ferroxidase complex shown in Figure 2 is important in discussing the mechanism of the ferroxidase reaction because it may be considered a valid model of the principal reactant. Invoking a single reactant structure likely oversimplifies the ferroxidase reaction. Both experimental and theoretical studies have demonstrated that the ferroxidase complexes are likely to possess several low-energy stable structures. But it is significant progress to have at least one structure upon which to

examine basic interaction with O_2 and from which other variations in ligand orientation may be explored.

Acknowledgment

The authors gratefully acknowledge the support of this research by the US National Science Foundation in the form of Grant No. 0 641 269.

References

[1] R.C. Binning, D.E. Bacelo, J. Biol. Inorg. Chem. 14 (2009) 1199.
[2] L. Toussaint, L. Bertrand, L. Hue, R.R. Crichton, J.P. Declercq, J. Mol. Biol. 365 (2007) 440. PDB ID: 2CEI.
[3] X. Liu, E.C. Theil, Acc. Chem. Res. 38 (2005) 167.
[4] N.D. Chasteen, P.M. Harrison, J. Struct. Biol. 126 (1999) 182.
[5] F. Bou-Abdallah, P. Arosio, P. Santambrogio, X. Yang, C. Janus-Chandler, N.D. Chasteen, Biochemistry 41 (2002) 11184.
[6] A. Treffry, Z. Zhao, M.A. Quail, J.R. Guest, P.M. Harrison, Biochemistry 36 (1997) 432.
[7] R.G. Pearson, J. Am. Chem. Soc. 85 (1963) 3533.
[8] B.L. d'Estaintot et al., J. Mol. Biol. 340 (2004) 277.
[9] T.J. Stillman et al., J. Mol. Biol. 307 (2001) 587.
[10] D.M. Lawson et al., Nature 349 (1991) 541.
[11] X. Liu, E.C. Theil, Proc. Natl. Acad. Sci. USA 101 (2004) 8557.
[12] J.K. Schwartz, P. Wei, K.H. Mitchell, B.G. Fox, E.I. Solomon, J. Am. Chem. Soc. 130 (2008) 7098.
[13] D.E. Bacelo, R.C. Binning, J. Phys. Chem. A 113 (2009) 1189.
[14] L. Noodleman, J. Chem. Phys. 74 (1981) 5737.
[15] R.C. Binning, D.E. Bacelo, J. Comput. Chem. 29 (2007) 716.
[16] R.C. Binning, D.E. Bacelo, Int. J. Quantum Chem. 109 (2009) 3533.
[17] A.D. Becke, Phys. Rev. A 38 (1988) 3098.
[18] J.P. Perdew, K. Burke, Y. Wang, Phys. Rev. B 54 (1996) 16533.
[19] B.J. Delley, J. Chem. Phys. 92 (1990) 508.
[20] B.J. Delley, J. Chem. Phys. 113 (2000) 7756.
[21] F. Bou-Abdallah, P. Arosio, S. Levi, C. Janus-Chandler, N.D. Chasteen, J. Biol. Inorg. Chem. 8 (2003) 489.
[22] J. Fetter, J. Cohen, D. Danger, J. Sanders-Loehr, Y. Ha, E.C. Theil, J. Biol. Inorg. Chem. 2 (1997) 652.